Macromolecules
ARTICLE

Macromolecules **2010**, *43*, 553–560 **553**
DOI: 10.1021/ma902049g

First Principles Prediction of The Propagation Rate Coefficients of Acrylic and Vinyl Esters: Are We There Yet?

Ching Yeh Lin, Ekaterina I. Izgorodina,† and Michelle L. Coote*

ARC Centre of Excellence for Free Radical Chemistry and Biotechnology, Research School of Chemistry, Australian National University, Canberra, ACT 0200, Australia. †Current address: School of Chemistry, Monash University, Victoria 3800, Australia.

Received September 14, 2009; Revised Manuscript Received November 5, 2009

ABSTRACT: High-level ab initio molecular orbital theory calculations have been used to calculate the rate coefficients and Arrhenius parameters for dimer models of the propagation steps for the free-radical homopolymerization of methyl acrylate and vinyl acetate at 298.15 K. Gas-phase Arrhenius parameters, as calculated under the hindered rotor model, showed large deviations from the corresponding solution-phase experimental data, because the stabilizing effect of hydrogen bonding in the transition structures of these reactions is much less significant in solution compared with the gas phase. This also leads to qualitative differences in the preferred transition state conformations in the respective phases, and it is therefore necessary to base all calculations (including the conformational analysis) on the solution-phase free energies. We find that chemically accurate values can be obtained via a thermodynamic cycle in which accurate G3(MP2)-RAD calculations in the gas phase are corrected to the solution phase using free energies of solvation, as computed by the COSMO-RS method. However, the use of DFT methods for the gas-phase energies and/or simple continuum models for the solvation energies can lead to errors of several orders of magnitude and should therefore be avoided for these types of reaction.

Introduction

The accurate and precise measurement of the rate and equilibrium constants of the various individual reactions of free-radical polymerization is crucial for the design and implementation of valid kinetic models for these complex processes. This has become particularly important with the development of controlled radical polymerization processes, as their success is often dependent upon striking a delicate balance of the rates of several competing reactions. Kinetic modeling offers the opportunity to study the effects of the reaction conditions, and the reactivities of the reagents themselves, on the overall outcome of the reaction. This information can then be used to develop simple guidelines for selecting (or designing) optimal control agents for the control of any specific monomer and for optimizing the other accompanying reaction conditions.

However, not only has the complexity of radical polymerization processes placed increased importance in the measurement of individual rate coefficients but also it has concurrently increased its difficulty. This is because experimental techniques, by necessity, can only measure the "observables" of a process, typically the overall reaction rate, the average molecular weight distributions, and the time dependent concentrations of some of the major species and/or major functional groups. These are then related to the individual rate coefficients by fitting some assumed model to the measured data. For simple homopolymerizations, the development of elegant techniques such as pulsed laser polymerization has made possible the measurement of the principal rate coefficients in a relatively model-free manner.[1] However, for more complex systems, such as controlled radical polymerization processes, the kinetic models themselves are less well established and further simplifying assumptions are in any case necessary to reduce the number of unknown model parameters. These model-based assumptions are a potentially large source of error in the rate coefficients obtained from experimental data.[2]

Given these difficulties, computational quantum chemistry offers an attractive complementary strategy for modeling free-radical polymerization processes as it can be used to calculate the rate and equilibrium constants of any individual chemical reaction directly, without recourse to model-based assumptions other than the requirements of quantum mechanics. However, as is well-known, the many-electron Schrödinger equation has no analytical solution and approximate numerical methods must be used. Although highly accurate methods exist, these are extremely computationally intensive, with their computational cost scaling rapidly with the size of the system. Applying quantum chemistry to polymerization processes therefore involves a compromise whereby the propagating radical and other polymeric species are modeled with corresponding oligomeric species, and so that these models can be as large and realistic as possible, lower-cost computational procedures are adopted. The use of oversimplified chemical models, and/or low-level quantum-chemical methods, can lead to large errors in the resulting kinetic data.

Nonetheless, aided by rapid and continuing increases in computer power, computational chemistry is rapidly establishing itself as a reliable and useful tool for the polymer field.[3] To date it has principally been used in mechanistic studies where qualitative or semiquantitative information is usually sufficient for practical purposes; however, progress has also been made toward the more ambitious goal of using computational chemistry to make quantitative predictions of rate and equilibrium constants. In a proof-of-principle study, we examined the chain length dependent propagation rate coefficients of vinyl chloride and acrylonitrile, showing that chain length effects converged to within a factor of

*Corresponding author. Fax: 61 2 6125 0750. E-mail: mcoote@rsc.anu.edu.au.

Published on Web 11/19/2009

2 of their long chain values once the propagating radical was modeled as a dimer.[4] When these dimer models were studied using high-level ab initio molecular theory calculations, the resulting (gas-phase) rate coefficients agreed with the corresponding (solution-phase) experimental values for the polymeric systems to within a factor of 2 in each case. For these systems, we showed that the inclusion of solvation effects, as modeled using a simple continuum model, had a negligible effect on the results. We have also taken this one step further and combined quantum-chemical predictions of the chain length dependent addition−fragmentation equilibrium in cyanoisopropyl dithiobenzoate mediated polymerization of styrene, with independent experimental rate coefficients for the addition step and the primary reactions in styrene polymerization, so as to simulate the initialization period of this reversible addition−fragmentation chain transfer (RAFT) process from first principles.[5] Our predicted concentration profiles for the various species, made without model fitting of any kind, showed excellent agreement with the independent experimental data,[6] measured under the same reaction conditions.

Despite this success, the treatment of more solvent sensitive systems remains problematic. Owing to the large size of the molecules involved, the majority of published computational studies have either neglected solvation effects altogether, or treated them using simple continuum models, such as CPCM[7] and PCM,[8] in which each solute molecule is simply embedded in an cavity surrounded by the relevant dielectric continuum. Although these computationally efficient models also include additional terms for the nonelectrostatic contributions of the solvent, such as dispersion, repulsion, and cavitation, they are generally thought to be reliable only when explicit solute−solvent interactions (such as hydrogen bonding) can be neglected.[9−11] It is also worth noting that results obtained with these models are very sensitive to the cavities used and these are generally optimized against experimental solvation energies for stable molecules, rather than transition structures.

To date, continuum models have been applied to radical polymerization processes with mixed success. We have used continuum model solvation energy calculations in conjunction with high-level ab initio molecular orbital theory calculations to predict chemically accurate *equilibrium constants* for reactions relevant to atom transfer radical polymerization (ATRP)[12] and RAFT.[13] We have also found that these procedures perform well for the prediction of redox potentials of a wide variety of open- and closed-shell species, including species relevant to ATRP and nitroxide mediated polymerization.[12,14] Applications of continuum models to polymerization *kinetics* have been more problematic. In an early study, Thickett and Gilbert used a simple PCM model to study the effect of solvent on acrylic acid propagation, confirming experimental observations[15] that aqueous solvation substantially lowers the reaction barrier.[16] However, it was noted that in this work that the levels of theory used in the gas- and solution-phase calculations were not accurate enough for quantitative predictions of the reaction rate. More recently, a DFT study of ethyl α-hydroxymethacrylate (EHMA) yielded a gas-phase propagation rate coefficient that differed from the corresponding solution-phase experimental values[17] by more than 5 orders of magnitude; when the effects of solvation were included in the calculations via a simple continuum model, the gap between theory and experiment actually widened to as much as 8 orders of magnitude.[18] However, it is again difficult to establish whether this large error stems primarily from the use of DFT methods for the gas-phase calculations, or the failure of the continuum model solvation energy corrections to account for the significant hydrogen bonding interactions in this system.

Given these problems, in the present work, we study the prototypical acrylic and vinyl esters, methyl acrylate and vinyl acetate, in order to explore whether chemical accuracy is achievable for these hydrogen-bonding monomers. To this end, we first benchmark the gas-phase electronic-structure calculations against gas-phase experimental data for related model systems, and then, using these procedures in combination with simple continuum solvation model methods, we compare the solution-phase predictions against corresponding experimental data. As part of this work, we also examine a new generation solvation method called COSMO-RS,[19] in order to determine whether this improves the accuracy of the calculations. During the course of our investigations, a gas-phase DFT study of methyl acrylate polymerization was published.[20] In this previous work, the predicted rate coefficients deviated from experiment by approximately 2 orders of magnitude, and as part of the present investigation we will explore whether these errors can be mitigated through the use of higher-level ab initio calculations and/or the inclusion of solvation energy corrections.

Scheme 1. Free Energy Cycle for the Dimer Propagation Reaction in Solution

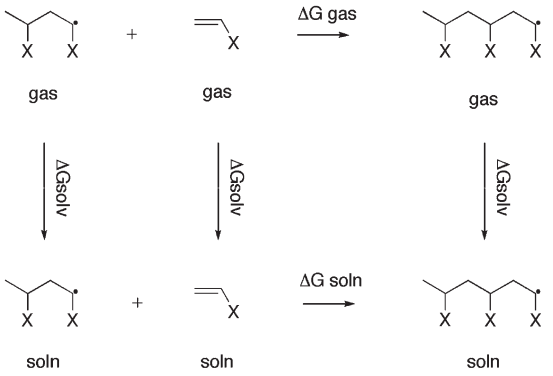

Computational Procedures

To calculate the rate coefficients of propagation reactions in the solution phase, we utilized the simple thermodynamic cycle shown in Scheme 1, whereby the free energies of each species in the solution phase were obtained as the sum of the corresponding gas-phase free energies and the free energies of solvation. In this way, we could make use of highly accurate *ab initio* procedures developed for the calculation of gas-phase species, and use the solvation model calculations only for the quantity they were directly parametrized for (i.e., the free energies of solvation rather than total free energies in solution). This also allows us to evaluate the accuracy of the gas- and solution-phase components of the calculations separately.

Gas-phase calculations were performed using the methodology we have previously developed for the chemically accurate prediction of propagation rate coefficients in free-radical polymerization.[4] Thus, geometries were optimized at the B3-LYP/6-31G(d) level of theory, and frequencies were also calculated at this level and scaled by the recommended[21] scale factors. Systematic conformational searching at a resolution of 120° was carried out to ensure all conformations were global rather than merely local minimum energy structures. Improved energies were calculated at the G3(MP2)-RAD level of theory, a high-level composite ab initio molecular orbital theory method that approximates CCSD(T) calculations with a large triple-ζ basis from calculations with a double-ζ basis set, via basis set corrections carried out the R(O)MP2 level of theory.[22] Where full G3(MP2)-RAD calculations were impractical, an ONIOM[23] approximation was used in which the core (designed to include the reaction center, all α-substituents, and any other substituents conjugated with it) was studied at G3(MP2)-RAD, and the remaining remote substituent effects were modeled at R(O)MP2/6-311+G(3df,2p). We have previously shown that this approach can reproduce full G3(MP2)-RAD

calculations to within chemical accuracy.[24] As part of this work, we have further confirmed the accuracy of this methodology for gas-phase rate calculations via an assessment study, in which we examined separately the effect of the level of theory for the geometry optimizations and the single-point energy calculations on the accuracy of the results, benchmarking the calculations against higher-level ab initio calculations and available gas-phase experimental data for related reactions (see the Results and Discussion section for further details).

Having obtained the geometries, frequencies and energies of each reactant and transition structure, gas-phase rate coefficients were calculated via the standard transition state theory eq 1.[25]

$$k(T) = \kappa(T)\frac{k_B T}{h}(c^\circ)^{1-m} e^{(-\Delta G^\ddagger/RT)} = \kappa(T)\frac{k_B T}{h}(c^\circ)^{1-m}\frac{Q_\ddagger}{\Pi Q_i} e^{(-\Delta E^\ddagger/RT)} \quad (1)$$

In this equation, $\kappa(T)$ is the tunneling correction factor, T is the absolute temperature, R is the universal gas constant (8.314 J mol^{-1} K^{-1}), k_B is the Boltzmann constant (1.380658×10^{-23} J mol^{-1} K^{-1}), h is the Planck's constant ($6.6260755 \times 10^{-34}$ J s), c° ($= P/RT$) is the standard unit of concentration (mol L^{-1}) and m is the molecularity of the reaction, $Q_\ddagger$ and Q_i are the molecular partition functions of the transition structure and reactant i respectively, $\Delta G^\ddagger$ is the Gibb's free energy of activation and $\Delta E^\ddagger$ is the 0 K, zero-point energy corrected energy barrier for the reaction. The value of c° depends on the standard-state concentration assumed in calculating the thermodynamic quantities (and translational partition function); in the present work, the (gas-phase) quantities were calculated for a mole of ideal gas at 298.15 K and 1 atm, and thus $c^\circ = 0.0409$ mol L^{-1}. The tunneling coefficient $\kappa(T)$ corrects for quantum effects in motion along the reaction path and can be assumed to be unity in the addition of carbon-centered radicals to alkenes, due to the large masses of the reacting groups.

Molecular partition functions (Q_i) and their associated thermodynamic functions (i.e., H, S, and G) were calculated using the optimized geometries and frequencies in conjunction with the standard textbook formulas, based on the statistical thermodynamics of an ideal gas under the harmonic oscillator rigid-rotor approximation.[26,27] These were then further corrected by treating all low frequency torsional modes as hindered internal rotations using the standard 1D-torsional eigenvalue summation (TES) method, applied at a 10° resolution, as described in a recent publication.[28] To mitigate the effects of coupling between the modes, we use the method of Van Cauter et al.[29] in which the harmonic oscillator approximation is applied to all $3N-6$ internal modes of a molecule, and the resulting vibrational partition function is then multiplied by a correction factor for each internal hindered rotor partition function. This factor is then calculated as the ratio of the hindered rotor partition function to the corresponding "pure" vibrational partition function, as calculated from second derivative of the rotational potential.

Solvation energies in bulk were calculated using the popular continuum model CPCM[7] in conjunction with both the UAKS and UAHF radii, and also the new generation method COSMO-RS.[19] These calculations were carried out using the theoretical procedures at which they were parametrized; namely, B3LYP/6-31+G(d) for CPCM-UAKS, HF/6-31+G(d) for CPCM-UAHF and BP/TZVP for COSMO-RS. As part of this work, we compared solvation energies obtained using geometries that were optimized in the solution phase versus those obtained using the gas-phase geometries. At each level of theory, free energies of each species in solution were obtained as the sum of the corresponding gas-phase free energy, the calculated free energy of solvation and a correction term, RT ln(24.46), to take account of the fact that the solvation energy is computed for the passage from 1 mol L^{-1} (g) to 1 mol L^{-1} (soln).[30] The overall solution phase free energy of activation was then used to calculate the rate coefficient via eq 1 as for the gas-phase calculations. In this equation, the standard unit of concentration (c°) has a value of 1 mol L^{-1} for solution-phase free energies. Since the solvation models are parametrized to calculate total free energies of solvation, rather than the individual enthalpic and entropic components, solution-phase Arrhenius parameters were obtained by repeating all calculations at 293 and 323 K and fitting the Arrhenius relationship to the resulting rate data.

All ab initio molecular orbital theory, density functional theory and solvation calculations were performed using Gaussian 03,[31] with following exceptions. URCCSD(T) calculations were performed in Molpro 2006.1,[32] and COSMO-RS calculations were performed in ADF,[33] using the implementation of Pye et al.[34] Calculations of partition functions were carried out using our in-house program TChem.[28,35]

Table 1. Comparison of Gas-Phase Theoretical and Solution-Phase Experimental Propagation Rate Coefficients (k_{298}; L mol^{-1} s^{-1}), Arrhenius Activation Energies (E_a; kJ mol^{-1}), and Frequency Factors (A; L mol^{-1} s^{-1}) for Methyl Acrylate and Vinyl Acetate Polymerization at 298.15 K[a]

	CH_2=CHCOOCH$_3$			CH_2=CHOCOCH$_3$		
level of theory	E_a	log(A)	log(k_{298})	E_a	log(A)	log(k_{298})
G3(MP2)-RAD (anti addition)	12.8	6.4	4.2	7.4	5.0	3.7
G3(MP2)-RAD (lowest conformer)	5.2	5.4	4.5	8.8	4.2	2.6
experimental value from ref 36	17.7	7.2	4.1	19.8	7.0	3.5
experimental value from ref 37				20.5	7.2	3.6

[a] G3(MP2)-RAD//B3-LYP/6-31G(d) calculations were performed dimer models of the propagating radical. Global minimum energy conformations were used for the reactants, and rates were calculated for both the lowest conformer of the transition structure and the corresponding anti addition conformers, as shown in Figure 1.

Results and Discussion

Gas-Phase Results. Propagation rate coefficients were calculated for the free-radical polymerization of the prototypical acrylic and vinyl esters, methyl acrylate and vinyl acetate. Initially, calculations were performed in the gas phase using the high-level *ab initio* methodology previously[4] shown to reproduce the propagation rate coefficients of acrylonitrile and vinyl chloride to within a factor of 2. Table 1 shows the resulting Arrhenius parameters and propagation rate coefficients for each monomer at 298.15 K, as calculated for the addition of a dimer propagating radical to the monomer, together with the corresponding experimental values.[36,37] From this table, we find that the agreement between theory and experiment is very disappointing. In both cases, while the propagation rate coefficients show very reasonable agreement with experiment (to within a factor of 2 for MA and an order of magnitude for VA), this is due to an unacceptably large cancellation of error in the barriers and frequency factors. In each case, the theoretical calculations significantly underestimate both the barrier and frequency factor, resulting in self-canceling errors of around 2−3 orders of magnitude in the resulting rate coefficients.

These discrepancies between theory and experiment raise serious questions about general applicability of quantum chemistry to radical polymerization processes, and it is therefore worth investigating the cause of these discrepancies, and whether they can be addressed by further improvements to the calculation procedure. To this end, we first test

Table 2. Effect of Level of Theory for the Geometry Optimizations on the Forming Bond Length in the Transition State (Å) and the Calculated Reaction Barrier (kJ mol^{-1})[a]

	methyl acrylate		vinyl acetate	
geometry level	forming bond	barrier	forming bond	barrier
B3LYP/6-31G(d)	2.299	14.1	2.312	11.4
B3LYP/6-311+G(3df,2p)	2.268	15.6	2.281	13.4
BMK/6-31G(d)	2.312	13.0	2.319	10.9
BMK/6-311+G(3df,2p)	2.283	13.5	2.288	10.8
MP2/6-31G(d)	2.256	15.4	2.248	11.3
MP2/6-311+G(3df,2p)	2.252	14.5	2.241	13.5
QCISD/6-31G(d)	2.248	13.7	2.259	11.5

[a] All barriers calculated using QCISD/6-31G(d) single points so that any differences represent only the effect of the geometry on the final results.

Table 3. Comparison of Gas-Phase Theoretical and Experimental Rate Coefficients (k_{298}; L mol^{-1} s^{-1}), Arrhenius Activation Energies (E_a; kJ mol^{-1}) and Frequency Factors (A; L mol^{-1} s^{-1}) at 298.15 K for Radical Addition to Alkenes [a]

	G3(MP2)-RAD			experimental[b]		
reaction	E_a	log(A)	log(k_{298})	E_a	log(A)	log(k_{298})
$^{\bullet}CH_2CH_3+CH_2{=}CH_2$	33.81	8.07	2.15	30.51	8.20	3.93
$^{\bullet}CH_2CH_3+CH_2{=}CHCN$	18.22	7.65	4.45	14.22	7.79	5.80
$^{\bullet}CH_2CH_3+CH_2{=}CHOCOCH_3$	30.01	7.20	1.94	28.85	7.89	3.85
$^{\bullet}CH_2CN+CH_2{=}CH_2$	37.41	8.09	1.53	37.81[c]	8.09[c]	1.46[c]

[a] All theoretical data calculated via standard transition state theory under the 1D-TES model. [b] Unless otherwise noted, experimental data taken from ref41. [c] Experimental data unavailable for this reaction; however, benchmark ab initio calculations (at the W1 level of theory[40]) were feasible and used instead.

the accuracy of our gas-phase rate calculations against gas-phase experimental data for a series of related model reactions, before examining whether the inclusion of solvation energies can diminish the discrepancies between theory and experiment.

Gas-Phase Assessment Study. The present calculations use state-of-the-art ab initio molecular theory methods, demonstrated to deliver chemical accuracy for a wide range of radical reactions.[3,5,12−14,24,38] They are based on full conformational searching for all species, and include hindered rotor corrections for all low frequency modes. Nonetheless, given the large discrepancies between theory and experiment in Table 1, it is worth examining further whether these gas phase calculations are capable of reproducing gas-phase experimental data. It is also worth testing whether the lower levels of theory used in the geometry optimizations are indeed sufficient for the present work. To this end, we carried out a small benchmarking study as follows.

First, to investigate the effect of level of theory for the geometry optimization on the accuracy of the results, geometries were optimized at a variety of levels of theory including low-level DFT methods with various basis sets, and various ab initio molecular orbital theory methods. As triple-ζ CCSD(T) calculations are impractical for geometry optimizations of species of this size, we have adopted the QCISD/6-31G(d) level of theory as our benchmark for Table 2. In previous testing for (smaller) prototypical radical addition reactions, this level of theory was shown to provide highly accurate geometries and frequencies.[39] Table 2 shows the calculated 0 K reaction barriers for methyl acrylate and vinyl acetate propagation, as calculated using a consistent level of theory for the energies, in this case QCISD/6-31G(d), but using geometries optimized at a variety of levels of theory. The forming bond lengths in the transition structures are also shown. So that high levels of theory could be used in the geometry optimizations, all calculations were carried out using unimer propagating radicals. As noted in our earlier studies of radical addition,[39] the DFT methods slightly overestimate the length of the forming bond in the transition state, compared with higher-level ab initio methods. However, this has a negligible effect on the resulting barrier height, which is virtually independent of the method and basis set used in the geometry optimizations. Thus, the results confirm that a low-cost level of theory such as B3-LYP/6-31G(d) is adequate for geometry optimizations for these reactions.

Second, having checked the geometry optimization method, we next used our G3(MP2)-RAD methodology to calculate the rate coefficients for ethyl radical addition to ethylene, acrylonitrile and vinyl acetate. These small model propagation reactions were chosen on the basis of the availability of *gas-phase* experimental data for benchmarking purposes. The addition of the delocalized radical $^{\bullet}CH_2CN$ to ethylene was also studied; for this system experimental data was unavailable but benchmarking calculations at the W1 level of theory[40] were possible instead. Table 3 shows the calculated Arrhenius parameters and rate coefficients at 298.15 K for each reaction, along with corresponding experimental data.[41,42] From this table we find that there is good agreement between theory and experiment, which further validates this methodology for gas-phase calculations.

Solvent Effects. Having discounted errors in the G3-(MP2)-RAD methodology for the gas-phase calculations, we next examined whether solvation effects could account for the discrepancy between theory and experiment. In this regard it is worth noting that, in their global minimum energy conformations in the gas phase, both propagation reactions proceed via gauche addition transition structures (see Figure 1). These crowded conformations appear to be stabilized via hydrogen bonding interactions between hydrogens on the terminal ester group of the propagating radical and the carbonyl of the monomer. In the case of vinyl acetate propagation, a second hydrogen bonding interaction between the carbonyl group of the propagating radical and the hydrogens of the monomer ester group also occurs. Similar hydrogen bonding interactions have been reported previously in studies of acrylate propagation kinetics,[18,43] and in the β-scission transition structures for certain xanthate-mediated polymerizations of vinyl acetate, where they are thought to contribute to the high activity of xanthates in reactions with this monomer.[44]

In the gas phase, these hydrogen-bonding interactions strongly stabilize the transition structure relative to the isolated reactants, thereby lowering the barrier. At the same time, they also reduce its flexibility (and hence its vibrational entropy), thereby lowering the frequency factor. To illustrate this qualitatively, we can re-evaluate the rate coefficients for each reaction using the corresponding anti addition conformations of the transition structures (as shown in Figure 1). For MA, the Arrhenius activation energy and frequency factor increase when the anti addition transition structure is studied, resulting in Arrhenius parameters that are closer to (but still different from) the experimental values (see Table 1). For VA, some hydrogen bonding is retained in the anti addition transition structure but the increase in vibrational flexibility leads to a modest increase in the frequency factor.[45] These illustrative calculations suggest that in the solution phase, where the energetic consequences of hydrogen bonding would be further diminished,[46] the

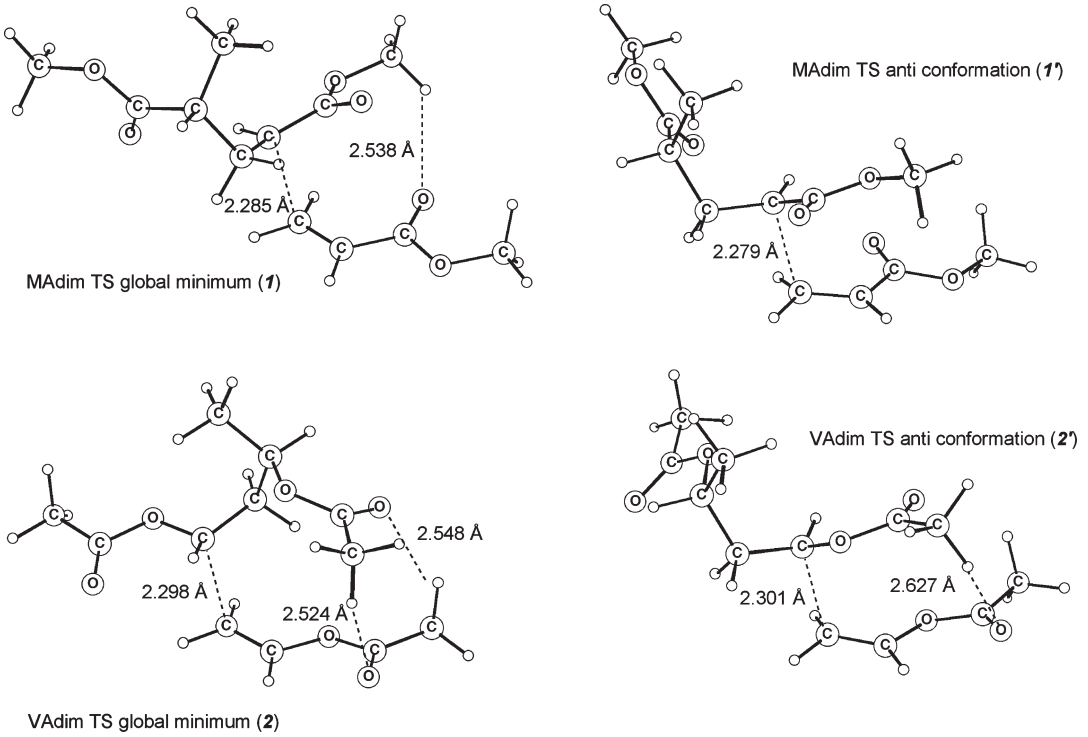

Figure 1. B3-LYP/6-31G(d) optimized gas-phase geometries of the minimum energy conformations of the transition structures for dimer models of the propagation step in methyl acrylate (**1**) and vinyl acetate (**2**) polymerization. The corresponding anti addition conformations (**1′** and **2′**) are also shown.

barrier and frequency factor should increase further, as observed experimentally.

To quantify the effects of solvation, we utilized the newly developed COSMO-RS method.[19] This method uses statistical thermodynamics to describe the interactions in a fluid as the local interaction of molecular surfaces, the interaction energies being quantified by the values of the two screening charge densities that form a molecule contact, in turn obtained from an initial continuum model calculation. The resulting energies from this method are expected to be more accurate than simple continuum model calculations because the real character of the solvent is taken into account. For the sake of comparison, we also performed calculations using the popular continuum solvation model CPCM,[7] as used successfully in our studies of the thermodynamics of ATRP[12] and RAFT[13] polymerization. The CPCM solvation model calculations were performed using both the UAKS and UAHF cavities, and all models were implemented at their recommended levels of theory. As noted above, the solution-phase free energies of activation were calculated using a simple thermodynamic cycle in which the reaction was studied using high-level ab initio molecular theory methods in the gas phase, and then corrected to the solution phase using the calculated solvation energies of each species.

Table 4 shows the 298.15 K solution phase Arrhenius parameters rate coefficients for each monomer, as calculated using the G3(MP2)-RAD gas-phase calculations in conjunction with solvation energies from each of the three solvation models (i.e., COSMO-RS, CPCM-UAHF, CPCM-UAKS). In this Table, OPT signifies that all geometries are reoptimized in the presence of solvent before calculating solvation energies; SP signifies that solvation energy calculations are performed as single point calculations on the gas-phase geometries. Although the former approach is normally preferable, this may not necessarily be the case for transition state optimizations, given that the methods used are parametrized for stable molecules only. The solution-phase experimental data is shown again for ease of comparison.

From Table 4, we find that the incorporation of solvation effects dramatically improves the agreement between the G3(MP2)-RAD calculations and experiment, consistent with the important role of solvent effects in this system. As expected, the solvation field decreases the relative importance of hydrogen bonding in the transition state, causing both the barrier and frequency factor to increase. Solvation also leads to a change in the preferred transition state for the reactions, with the anti addition pathways, which are less crowded but less subject to hydrogen bonding interactions, now having lower free energies (and hence faster rate coefficients) than those for gauche addition. Among the levels of theory tested, use of the most sophisticated solvation method, COSMO-RS, provides the best agreement between theory and experiment, predicting barriers to within 4 kJ mol^{-1} or better of the experimental results, and rate coefficients to within an order of magnitude or better. The results based on CPCM solvation energies tend to overestimate the barriers, and underestimate the rate coefficients accordingly. This poor performance contrasts with their promising results for reaction *thermodynamics*, and probably stems from the fact that these methods have not been parametrized for transition structures. We did not have access to the software required to perform geometry optimizations in the presence of solvent using COSMO-RS; however, reoptimization of the geometry in solution prior to calculation of the solvation energy had a relatively minor effect on the CPCM results. Overall, the results shown here confirm the important role of solvent effects in these reactions, and suggest that these can be modeled with reasonable accuracy using COSMO-RS, at least for the present systems.

Comparison with Earlier Work. Finally, it is worth comparing the present ab initio results with those from an earlier DFT study of acrylate monomers.[20] The Arrhenius parameters for methyl acrylate propagation, as calculated using

Table 4. Comparison of Solution-Phase Theoretical and Experimental Propagation Rate Coefficients (k_{298}; L mol^{-1} s^{-1}), Arrhenius Activation Energies (E_a; kJ mol^{-1}) and Frequency Factors (A; L mol^{-1} s^{-1}) for Methyl Acrylate and Vinyl Acetate Polymerization at 298.15 K[a]

	CH_2=CHCOOCH$_3$			CH_2=CHOCOCH$_3$		
level of theory	E_a	log(A)	log(k_{298})	E_a	log(A)	log(k_{298})
			Anti-Addition			
CPCM-UAHF HF/6-31+G(d) (SP)	34.7	8.2	2.1	31.4	6.6	1.1
CPCM-UAHF HF/6-31+G(d) (OPT)	31.5	7.7	2.2	29.8	6.4	1.2
CPCM-UAKS B3LYP/6-31+G(d) (SP)	31.4	6.6	1.1	30.6	6.4	1.1
CPCM-UAKS B3LYP/6-31+G(d) (OPT)	31.6	7.7	2.2	28.4	6.3	1.4
COSMO-RS BP/TZVP (SP)	21.8	7.5	3.7	17.6	6.1	3.0
			Gauche Addition			
CPCM-UAHF HF/6-31+G(d) (SP)	29.9	7.1	1.9	35.6	5.8	−0.5
CPCM-UAHF HF/6-31+G(d) (OPT)	27.4	6.7	1.9	33.5	5.8	−0.1
CPCM-UAKS B3LYP/6-31+G(d) (SP)	32.8	7.6	1.8	34.9	5.6	−0.5
CPCM-UAKS B3LYP/6-31+G(d) (OPT)	27.5	6.7	1.9	30.3	5.6	0.3
COSMO-RS BP/TZVP (SP)	17.6	6.5	3.4	20.2	5.4	1.9
			Experiment			
experimental value in ref 36	17.7	7.2	4.1	19.8	7.0	3.5
experimental value in ref 37				20.5	7.2	3.6

[a] G3(MP2)-RAD//B3-LYP/6-31G(d) calculations were performed dimer models of the propagating radical for both the gauche addition and anti addition conformers shown in Figure 1. SP signifies that gas-phase geometries were used for calculation of solvation energies; OPT signifies geometries were reoptimized in solution.

Table 5. Comparison of MPWB1K and G3(MP2)-RAD Propagation Rate Coefficients (k_{298}; L mol^{-1} s^{-1}), Arrhenius Activation Energies (E_a; kJ mol^{-1}) and Frequency Factors (A; L mol^{-1} s^{-1}) for Methyl Acrylate Propagation[a]

	gas phase			solution phase[b]		
level of theory	E_a	log(A)	log(k_{298})	E_a	log(A)	log(k_{298})
MPWB1K (ref 20)	24.3	6.5	2.3	33.3	6.3	1.7
MPWB1K (anti addition)	30.6	5.9	0.5	39.6	6.9	0.0
MPWB1K (gauche addition)	22.8	5.1	1.1	35.2	6.2	0.0
G3(MP2)-RAD (anti addition)	12.8	6.4	4.2	21.8	7.5	3.7
G3(MP2)-RAD (gauche addition)	5.2	5.4	4.5	17.6	6.5	3.4
experimental value in ref 36				17.7	7.2	4.1

[a] Calculated for a dimer model of the propagating radical for both the (gas-phase) global minimum gauche addition transition structure, and the anti addition transition structures shown in Figure 1. The ref 20 MPWB1*K*/6-311+G(3df,2p)//B3LYP/6-31+G(d) gas-phase Arrhenius parameters are taken from Table 6 of ref 20; solvation corrections have then been calculated and used to adjust the data to the solution phase. It is not specified in this earlier work, whether the Arrhenius parameters refer to the unimer, dimer, trimer or tetramer model; however, the Arrhenius parameters yield rate coefficients consistent with the (almost identical) unimer and dimer model propagation rate coefficients in Table 5 of the same paper. The dimer model transition state conformation in this earlier work is not shown in ref 20, however, based on the unimer model conformations shown, it would appear that a slightly higher-energy transition state conformation was adopted in this earlier work. We have therefore additionally recalculated the propagation rate coefficients at the MPWB1*K*/6-311+G(3df,2p)//B3LYP/6-31+G(d) level using the same geometries as the present work to allow for consistent comparison. [b] Solvation effects calculated using COSMO-RS BP/TZVP.

the MPWB1*K*/6-311+G(3df,2p)//B3-LYP/6-31+G(d) level of theory in this earlier study, are shown in Table 5, along with the corresponding rate coefficient at 298.15 K, as calculated using these values. In performing this comparison, we noticed that the transition state conformation used in this earlier work is not the global minimum in the gas phase; hence results were also recalculated at this level of theory on the global minimum structure for consistent comparison with our G3(MP2)-RAD data. Solvation corrections were also added to the MPWB1*K*/6-311+G(3df,2p)//B3-LYP/6-31+G(d) calculations using the best-performing solvent model, COSMO-RS, and the corresponding solution-phase results are also shown in Table 5 along with the corresponding G3(MP2)-RAD values.

From Table 5, it is seen that the MPWB1*K*/6-311+G(3df,2p)//B3-LYP/6-31+G(d) level of theory yields energy barriers, and hence rate coefficients, that are very different to those at G3(MP2)-RAD. When the gas-phase results for the same gauche addition transition state conformation are compared, MPWB1K overestimates the reaction barrier by 17.6 kJ mol^{-1} compared with G3(MP2)-RAD. This overestimation brings the straight gas-phase barrier at the MPWB1K level much closer to the solution-phase experimental value. However, once solvation energy corrections are made, there is a substantial discrepancy between theory and experiment at this level of theory. It seems likely that MPWB1K may be underestimating the strength of the hydrogen bonding interactions and in this way fortuitously causing the gas-phase results to resemble the solution-phase experimental data in this particular case. In support of this, we note that when we examined the performance of the MPWB1K method for the model reactions in Table 3, there was much closer agreement between the two levels of theory (the MADs are 3.4 and 2.2 kJ mol^{-1} for MPWB1K and G3(MP2)-RAD, respectively; see Table S3 of the Supporting Information for full results). The improved performance in this case is presumably because hydrogen bonding and other dispersion interactions do not play a major role in these reactions. This large variability in the performance of DFT methods such as MPWB1K has been demonstrated elsewhere for a variety of simple organic reactions, where for some reactions errors can range from a few kilojoules up to tens of kilojoules as the substituents are changed.[4,24,47] It is this variability and unpredictability in their performance that makes these low-cost

procedures unsuitable as universal levels of theory for chemically accurate calculations.

Conclusion

In conclusion, the use of quantum chemistry to predict chemically accurate propagation rate coefficients in free-radical polymerization is a challenge for solvent sensitive monomers such acrylic and vinyl esters. In particular, the use of standard gas-phase calculations to study the solution-phase reactions can lead to large errors in the quantitative and even qualitative conclusions, even when high levels of theory are used. Specifically, such calculations tend to overestimate the stabilizing effect of hydrogen bonding in the transition structures of these reactions, leading to barriers and frequency factors that are much higher than their equivalent reactions in solution. For the same reason, the lowest energy reaction pathways in the gas phase feature crowded gauche addition transition structures in which hydrogen-bonding interactions are maximized, whereas in solution, the reactions actually proceed via less crowded anti addition transition structures.

Fortunately, for these systems at least, chemically accurate solution-phase results are possible using a thermodynamic cycle in which accurate G3(MP2)-RAD calculations in the gas phase are corrected to the solution phase using free energies of solvation, as computed by the COSMO-RS method. Using this methodology, the quantum-chemical predictions for both methyl acrylate and vinyl acetate propagation reproduce the corresponding experimental barriers to within 4 kJ mol^{-1}, with predictions of frequency factors and rate coefficients to within an order of magnitude. Further testing of this methodology on a broader range of systems is necessary, but the present results certainly provide encouragement that chemically accurate calculations are feasible for radical polymerization processes.

Acknowledgment. We gratefully acknowledge support from the Australian Research Council under their Centres of Excellence program, and generous allocations of computing time on the National Facility of the National Computational Infrastructure.

Supporting Information Available: A scheme showing the chemical structures of all species studied and tables of complete optimized geometries, corresponding total energies, entropies, enthalpies, rotational barriers and solvation energies for all species and further comparisons of MPWB1K and G3(MP2)-RAD results. This material is available free of charge via the Internet at http://pubs.acs.org.

References and Notes

(1) (a) Coote, M. L.; Zammit, M. D.; Davis, T. P. *Trends Polym. Sci.* **1996**, *4*, 189–196. (b) van Herk, A. M. *Macromol. Theory Simul.* **2000**, *9*, 433–441. (c) Beuermann, S.; Buback, M. *Prog. Polym. Sci.* **2002**, *27*, 191–254. (d) Barner-Kowollik, C.; Buback, M.; Egorov, M.; Fukuda, T.; Goto, A.; Olaj, O. F.; Russell, G. T.; Vana, P.; Yamada, B.; Zetterlund, P. B. *Prog. Polym. Sci.* **2005**, *30*, 605–643.

(2) For a discussion of this problem, see for example: Barner-Kowollik, C.; Coote, M. L.; Davis, T. P.; Radom, L.; Vana, P. *J. Polym. Sci. A Polym. Chem.* **2003**, *41*, 2828–2832.

(3) For recent reviews of applications in free-radical polymerization, see for example: (a) Coote, M. L. *Macromol. Theory Simul.* **2009**, *18*, 388–400. (b) Coote, M. L.; Krenske, E. H.; Izgorodina, E. I. *Macromol. Rapid Commun.* **2006**, *27*, 473–497.

(4) Izgorodina, E. I.; Coote, M. L. *Chem. Phys.* **2006**, *324*, 96–110.

(5) Coote, M. L.; Izgorodina, E. I.; Krenske, E. H.; Busch, M.; Barner-Kowollik, C. *Macromol. Rapid Commun.* **2006**, *27*, 1015–1022.

(6) McLeary, J. B.; Calitz, F. M.; McKenzie, J. M.; Tonge, M. P.; Sanderson, R. D.; Klumperman, B. *Macromolecules* **2004**, *37*, 2383–2394.

(7) (a) Klamt, A.; Schueuermann, G. *J. Chem. Soc., Perkin Trans. 2* **1993**, 799–805. (b) Cossi, M.; Rega, N.; Scalmani, G.; Barone, V. *J. Comput. Chem.* **2003**, *24*, 669–681.

(8) Miertus, S.; Scrocco, E.; Tomasi, J. *J. Chem. Phys.* **1981**, *55*, 117–129.

(9) Tomasi, J. *Theor. Chem. Acc.* **2004**, *112*, 184–203.

(10) Takano, Y.; Houk, K. N. *J. Chem. Theory Comput.* **2005**, *1*, 70–77.

(11) See for example: Ho, J.; Coote, M. L. *J. Chem. Theory Comput.* **2009**, *5*, 295–306.

(12) (a) Lin, C. Y.; Coote, M. L.; Gennaro, A.; Matyjaszewski, K. *J. Am. Chem. Soc.* **2008**, *130*, 12762–12774. (b) Tang, W.; Kwak, Y.; Braunecker, W.; Tsarevsky, N. V.; Coote, M. L.; Matyjaszewski, K. *J. Am. Chem. Soc.* **2008**, *130*, 10702–10713.

(13) Lin, C. Y.; Coote, M. L. *Aust. J. Chem.* **2009**, in press. DOI: 10.1071/CH09269.

(14) See for example: (a) Namazian, M.; Coote, M. L. *J. Phys. Chem. A* **2007**, *111*, 7227–7232. (b) Hodgson, J. L.; Namazian, M.; Bottle, S. E.; Coote, M. L. *J. Phys. Chem. A* **2007**, *111*, 13595–13605. (c) Namazian, M.; Zare, H. R.; Coote, M. L. *Biophys. Chem.* **2008**, *132*, 64–68. (d) Namazian, M.; Siahrostami, S.; Coote, M. L. *J. Fluorine Chem.* **2008**, *129*, 222–225. (e) Blinco, J. P.; Hodgson, J. L.; Morrow, B. J.; Walker, J. R.; Will, G. D.; Coote, M. L.; Bottle, S. E. *J. Org. Chem.* **2008**, *73*, 6763–6771. (f) Zare, H.; Eslami, M.; Namazian, M.; Coote, M. L. *J. Phys. Chem. B* **2009**, *113*, 8080–8085.

(15) Beuermann, S.; Buback, M.; Hesse, P.; Kuchta, F.-D.; Lacik, I.; Van Herk, A. M. *Pure Appl. Chem.* **2007**, *79* (8), 1463–1469.

(16) Thickett, S. C.; Gilbert, R. G. *Polymer* **2004**, *45*, 6993–6999.

(17) Morrison, D. A.; Davis, T. P. *Macromol. Chem. Phys.* **2000**, *201*, 2128–2137.

(18) Degirmenci, I.; Avci, D.; Aviyente, V.; Van Cauter, K.; Van Speybroeck, V.; Waroquier, M. *Macromolecules* **2007**, *40*, 9590–9602.

(19) (a) Klamt, A. *J. Phys. Chem.* **1995**, *99*, 2224–2235.(b) Klamt, A. *COSMO-RS: From Quantum Chemistry to Fluid Phase Thermodynamics and Drug Design*; Elsevier Science Ltd.: Amsterdam, The Netherlands, 2005. (c) Klamt, A.; Jonas, V.; Burger, T.; Lohrenz, J. C. W. *J. Phys. Chem. A* **1998**, *102*, 5074–5085.

(20) Degirmenci, I.; Aviyente, V.; Van Speybroeck, V.; Waroquier, M. *Macromolecules* **2009**, *42*, 3033–3041.

(21) Scott, A. P.; Radom, L. *J. Phys. Chem.* **1996**, *100*, 16502–16513.

(22) Henry, D. J.; Sullivan, M. B.; Radom, L. *J. Chem. Phys.* **2003**, *118*, 4849–4860.

(23) (a) Vreven, T.; Morokuma, K. *J. Chem. Phys.* **1999**, *111*, 8799 – 8803. (b) Vreven, T.; Morokuma, K. *J. Comput. Chem.* **2000**, *21*, 1419–1432.

(24) See for example: (a) Izgorodina, E. I.; Coote, M. L. *J. Phys. Chem. A* **2006**, *110*, 2486–2492. (b) Izgorodina, E. I.; Brittain, D. R. B.; Hodgson, J. L.; Krenske, E. H.; Lin, C. Y.; Namazian, M.; Coote, M. L. *J. Phys. Chem. A* **2007**, *111*, 10754–10768. (c) Lin, C. Y.; Hodgson, J. L.; Namazian, M.; Coote, M. L. *J. Phys. Chem. A* **2009**, *113*, 3690–3697.

(25) See for example: (a) Truhlar, D. G.; Garrett, B. C.; Klippenstein, S. J. *J. Phys. Chem.* **1996**, *100*, 12771–12800.

(26) See for example: (a) Stull, D. R.; Westrum, E. F., Jr.; Sinke, G. C. *The Thermodynamics of Organic Compounds*; John Wiley & Sons: New York, 1969. (b) Robinson, P. J. *J. Chem. Educ.* **1978**, *55*, 509–510. (c) Steinfeld, J. I.; Francisco, J. S.; Hase, W. L. *Chemical Kinetics and Dynamics*; Prentice Hall: Englewood Cliffs, NJ, 1989.

(27) These formulae are outlined in full in the Supporting Information of an earlier publication in this journal: Coote, M. L.; Radom, L. *Macromolecules* **2004**, *37*, 590–596.

(28) Lin, C. Y.; Izgorodina, E. I.; Coote, M. L. *J. Phys. Chem. A* **2008**, *112*, 1956–1964.

(29) Van Cauter, K.; Van Speybroeck, V.; Vansteenkiste, P.; Reyniers, M.-F.; Waroquier, M. *ChemPhysChem* **2006**, *7*, 131–140.

(30) Liptak, M. D.; Gross, K. G.; Seybold, P. G.; Feldgus, S.; Shields, G. C. *J. Am. Chem. Soc.* **2002**, *124*, 6421–6427.

(31) Frisch, M. J.; Trucks, G. W.; Schlegel, H. B.; Scuseria, G. E.; Robb, M. A.; Cheeseman, J. R.; Montgomery, J. A., Jr.; Vreven, T.; Kudin, K. N.; Burant, J. C.; Millam, J. M.; Iyengar, S. S.; Tomasi, J.; Barone, V.; Mennucci, B.; Cossi, M.; Scalmani, G.; Rega, N.; Petersson, G. A.; Nakatsuji, H.; Hada, M.; Ehara, M.; Toyota, K.; Fukuda, R.; Hasegawa, J.; Ishida, M.; Nakajima, T.; Honda, Y.; Kitao, O.; Nakai, H.; Klene, M.; Li, X.; Knox, J. E.; Hratchian, H. P.; Cross, J. B.; Adamo, C.; Jaramillo, J.; Gomperts, R.; Stratmann, R. E.; Yazyev, O.; Austin, A. J.; Cammi, R.; Pomelli, C.; Ochterski, J. W.; Ayala, P. Y.; Morokuma, K.; Voth, G. A.; Salvador, P.; Dannenberg, J. J.; Zakrzewski, V. G.; Dapprich, S.;

Daniels, A. D.; Strain, M. C.; Farkas, O.; Malick, D. K.; Rabuck, A. D.; Raghavachari, K.; Foresman, J. B.; Ortiz, J. V.; Cui, Q.; Baboul, A. G.; Clifford, S.; Cioslowski, J.; Stefanov, B. B.; Liu, G.; Liashenko, A.; Piskorz, P.; Komaromi, I.; Martin, R. L.; Fox, D. J.; Keith, T.; Al-Laham, M. A.; Peng, C. Y.; Nanayakkara, A.; Challacombe, M.; Gill, P. M. W.; Johnson, B.; Chen, W.; Wong, M. W.; Gonzalez, C.; Pople, J. A. *Gaussian 03, Revision B.03*; Gaussian, Inc.: Pittsburgh PA, 2003.

(32) MOLPRO, version 2006.6, a package of ab initio programs. Werner, H.-J.; Knowles, P. J.; Lindh, R.; Manby, F. R.; Schütz, M.; Celani, P.; Korona, T.; Rauhut, G.; Amos, R. D.; Bernhardsson, A.; Berning, A.; Cooper, D. L.; Deegan, M. J. O.; Dobbyn, A. J.; Eckert, F.; Hampel, C.; Hetzer, G.; Lloyd, A. W.; McNicholas, S. J.; Meyer, W.; Mura, M. E.; Nicklass, A.; Palmieri, P.; Pitzer, R.; Schumann, U.; Stoll, H.; Stone, A. J.; Tarroni, R.; Thorsteinsson, T. See: http://www.molpro.net.

(33) Louwen, J. N.; Pye, C.; Lenthe, E. v. ADF2008.01 COSMO-RS, SCM, *Theoretical Chemistry*: Vrije Universiteit: Amsterdam, The Netherlands, http://www.scm.com, 2008.

(34) Pye, C. C.; Ziegler, T.; van Lenthe, E.; Louwen, J. N. *Can. J. Chem.* **2009**, *87*, 790–797.

(35) This program is freely available from http://rsc.anu.edu.au/∼cylin/scripts.html.

(36) Manders, B. G. Ph.D. Thesis, Eindhoven University of Technology: Eindhoven, The Netherlands, **1997**.

(37) Hutchinson, R. A.; Paquet, D. A., Jr.; McMinn, J. H.; Beuermann, S.; Fuller, R. E.; Jackson, C. *DCHEMA Monogr*. **1995**, *131*, 467–492.

(38) Lobachevsky, S.; Schiesser, C. H.; Lin, C. Y.; Coote, M. L. *J. Phys. Chem. A* **2008**, *112*, 13622–13627.

(39) See, for example: (a) Gómez-Balderas, R.; Coote, M. L.; Henry, D. J.; Radom, L. *J. Phys. Chem. A* **2004**, *108*, 2874–2883. (b) Coote, M. L.; Wood, G. P. F.; Radom, L. *J. Phys. Chem. A* **2002**, *106*, 12124–12138.

(40) Martin, J. M. L.; De Oliveira, G. J. *J. Chem. Phys*. **1999**, *111*, 1843–1856.

(41) National Institute of Standards and Technology (NIST), Chemical Kinetics Database on the Web, Standard Reference Database 17, Version 7.0 (Web Version), Release 1.2 http://kinetics.nist.gov/index.php

(42) Luo, Y.-R., *Handbook of Bond Dissociation Energies in Organic Compounds*. CRC Press: Boca Raton, FL, 2003.

(43) See for example: Buback, M.; Müller, E. *Macromol. Chem. Phys.* **2007**, *208*, 581–593.

(44) (a) Coote, M. L.; Radom, L. *Macromolecules* **2004**, *37*, 590–596. (b) Coote, M. L.; Izgorodina, E. I.; Cavigliasso, G. E.; Roth, M.; Busch, M.; Barner-Kowollik, C. *Macromolecules* **2006**, *39*, 4585–4591.

(45) The energy of the anti addition transition state is 7.4 kJ mol^{-1} above the gauche addition structure; however, its increased vibrational energy results in an enthalpy at 298.15 K (and hence Arrhenius activation energy) that is slightly lower.

(46) On the basis of a crude electrostatic model, the strength of hydrogen bond should be inversely related to the dielectric constant of the medium. The reality is of course more complex but it is nonetheless generally observed that the strength of hydrogen bonding interactions decreases significantly as the polarity of the reaction medium increases. For a discussion, see for example: Chen, J.; McAllister, M. A.; Lee, J. K.; Houk, K. N. *J. Org. Chem.* **1998**, *63*, 4611–4619.

(47) See for example: (a) Choi, C. C.; Kertesz, M.; Karpfen, A. *Chem. Phys. Lett*. **1997**, *276*, 266–268. (b) Curtiss, L. A.; Raghavachari, K.; Redfern, P. C.; Pople, J. A. *J. Chem. Phys*. **2000**, *112*, 7374–7383. (c) Woodcock, H. L.; Schaefer, H. F., III; Schreiner, P. R. *J. Phys. Chem. A* **2002**, *106*, 11923–11931. (d) Izgorodina, E. I.; Coote, M. L.; Radom, L. *J. Phys. Chem. A* **2005**, *109*, 7558–7566. (e) Check, C. E.; Gilbert, T. M. *J. Org. Chem*. **2005**, *70*, 9828–9834. (f) Grimme, S. *Angew. Chem., Int. Ed.* **2006**, *45*, 4460–4464. (g) Schreiner, P. R.; Fokin, A. A.; Pascal, R. A., Jr.; de Meijere, A. *Org. Lett*. **2006**, *8*, 3635–3638. (h) Wodrich, M. D.; Corminbœf, C.; von Ragué Schleyer, P. *Org. Lett*. **2006**, *8*, 3631–3634. (i) Wodrich, M. D.; Corminbœf, C.; Schreiner, P. R.; Fokin, A. A.; von Ragué Schleyer, P. *Org. Lett*. **2007**, *9*, 1851–1854. (j) Grimme, S.; Steinmetz, M.; Korth, M. *J. Chem. Theory Comput*. **2007**, *3*, 42–45. (k) Schreiner, P. R. *Angew. Chem., Int. Ed.* **2007**, *46*, 4217–4219. (l) Brittain, D. R. B.; Lin, C. Y.; Gilbert, A. T. B.; Izgorodina, E. I.; Gill, P. M. W.; Coote, M. L. *Phys. Chem. Chem. Phys*. **2009**, *11*, 1138–1142.